ISSN 0023-1584, Kinetics and Catalysis, 2012, Vol. 53, No. 3, pp. 384–394. © Pleiades Publishing, Ltd., 2012.
Original Russian Text © Luu Cam Loc, Nguyen Manh Huan, N.A. Gaidai, Ho Si Thoang, Yu.A. Agafonov, N.V. Nekrasov, A.L. Lapidus, 2012, published in Kinetika i Kataliz, 2012, Vol. 53, No. 3, pp. 400–409.

Kinetics of Carbon Monoxide Methanation on Nickel Catalysts

Luu Cam Loc[a], Nguyen Manh Huan[a], N. A. Gaidai[b], Ho Si Thoang[a], Yu. A. Agafonov[b], N. V. Nekrasov[b], and A. L. Lapidus[b]

[a] *Institute of Chemical Technology, Vietnamese Academy of Science and Technology, Ho Chi Minh City, Vietnam*
[b] *Zelinsky Institute of Organic Chemistry, Russian Academy of Sciences, Moscow, 119991 Russia*
e-mail: gaidai@server.ioc.ac.ru

Received April 5, 2011

Abstract—The kinetics of CO methanation in excess H_2 on CaO- and CeO_2-doped nickel catalysts supported on Al_2O_3 and TiO_2 was studied at atmospheric pressure in a temperature range of 180–240°C. It was found that the same rational fractional rate equation corresponding to the reaction taking place at high surface coverages, is valid for all of the catalysts. The activity of nickel catalysts in the methanation reaction and their adsorption capacity with respect to reaction mixture components depend on the nature of the support and dopants.

DOI: 10.1134/S0023158412030093

INTRODUCTION

The kinetics of CO methanation on nickel catalysts was intensively studied in the 1960s and 1970s, when the use of synthetic natural gas became of considerable interest. The rate equations proposed for this reaction on different nickel catalysts can be divided into zero order equations [1–5], power equations [5–15], and Langmuir–Hinshelwood equations [15–25]. In the power equations, the orders of reaction with respect to hydrogen and CO vary in the ranges from 0.5 to 1.8 and from –0.87 to 1.0, respectively. The partial pressure of water vapor, which inhibits the process, also appear in the power rate equations of methanation [7, 9, 13].

The form of the rate equations of CO methanation depends on the ratio of the initial components and on temperature. For examples, in a study performed by Sehested et al. [5] on a $Ni/MgAl_2O_4$ catalyst, the order of reaction with respect to CO was unity at low partial pressures of CO, zero at high partial pressures, and lower than unity but positive at medium partial pressures. In the cited study, the first order with respect to CO was observed on nickel wire, and it was assumed that the slow step of the process is the dissociation of CO ($CO_{ads} = C_{ads} + O_{ads}$). Ho and Harriott [15] found that the order of the reaction with respect to CO on a Ni/SiO_2 catalyst at high pressures of CO varied from zero to small negative values. At high partial pressures of hydrogen and high temperatures, the order of the reaction with respect to CO became positive, and the order with respect to H_2 varied from 0.5 to 1.0 and increased with increasing P_{CO} and decreasing P_{H_2}. It was assumed that, at medium partial pressures of CO and H_2, the slow step is $CO_{ads} + 2H_{ads} = C_{ads} + H_2O$, and the experimental data were best fitted to a Langmuir–Hinshelwood equation. The Langmuir–Hinshelwood equations suggested for the methanation rate, which were derived under the assumption that the surface of nickel catalysts is either homogeneous or inhomogeneous, have different forms: the orders with respect to CO and H_2 in the numerator of the equation vary from 0.5 to 1.0, and the power of the denominator varies from 0.5 to 3.0.

In principle, under certain process conditions, the Langmuir–Hinshelwood equations can be approximated by simpler power equations. The published kinetic description [26, 27] of CO methanation on Ni/Al_2O_3 in the unsteady-state region assumes that strongly adsorbed species, including CO, participate in the reaction. In a number of publications [12, 16, 18, 19, 23], a maximum was detected in the dependence of the rate of methane formation on P_{CO}. The absence of this maximum can be explained by an insufficiently wide interval of the variation of the partial pressures of parent substances.

The form of the rate equation does not allow one to unambiguously judge the nature of the slow step of the process because the same rate equation can be derived based on different assumptions about the slow step of the reaction and different rate equations can correspond to the same slow step (for example, at different adsorbate coverages of the surface) [28].

Thus, the kinetics of CO methanation on nickel catalysts can be described by various equations ranging from simple power equations to fractional rational equations. The development of an adequate kinetic model is of considerable importance because a rate equation can serve as a basis for designing industrial

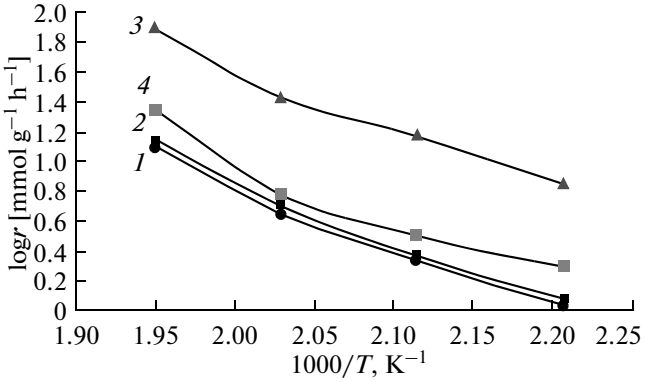

Fig. 1. The temperature dependence of the reaction rate in the Arrhenius coordinates for the following catalysts: (*1*) NiTi, (*2*) NiAl, (*3*) NiCaAl, and (*4*) NiCeAl.

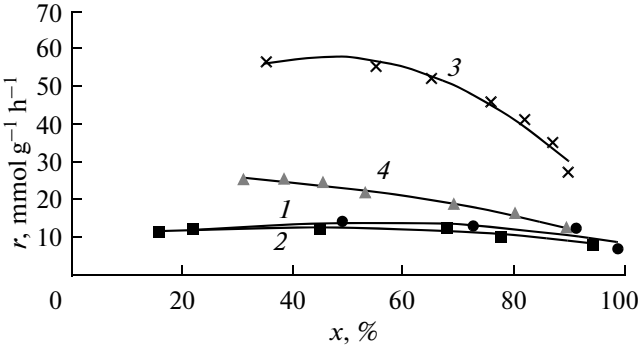

Fig. 2. Dependence of the reaction rate on the CO conversion at 240°C, $P^0_{H_2}$ = 333 hPa, and P^0_{CO} = 10 hPa on the following catalysts: (*1*) NiTi, (*2*) NiAl, (*3*) NiCaAl, and (*4*) NiCeAl.

reactors and for optimizing the operation conditions. The purpose of this work was to study the kinetics of CO methanation on different supported nickel catalysts and the effect of calcium and cerium dopants on the reaction kinetics. Previously, we used isotopic and unsteady-state methods to investigate the mechanism of CO methanation [29] and proposed a step-by-step reaction scheme; however, comprehensive data on the kinetics of the reaction are required for solving the problem of the nature of the slow step.

EXPERIMENTAL

The reaction kinetics was studied in a flow-circulation sealed glass system at atmospheric pressure. The experiments were performed at the initial partial pressures P^0_{CO} = 5–30 hPa and $P^0_{H_2}$ = 167–667 hPa in the presence of methane ($P^0_{CH_4}$ to 30 hPa) and water vapor ($P^0_{H_2O}$ to 43.3 hPa). The temperature range was 180–240°C, and the gas mixture flow rate was varied from 3 to 48 L/h. Under these conditions, methanation was almost irreversible. The CO conversion (x) varied from 5.6 to 97.3%. Nitrogen was used as the diluent.

As previously [29], the experiments were carried out on the following nickel catalysts: 7.5 wt % NiO/TiO_2 (NiTi), 37.5% NiO/γ-Al_2O_3 (NiAl), (37.5% NiO +10.2% CaO)/γ-Al_2O_3 (NiCaAl), and (37.5% NiO + 0.1% Ce_2O_3)/γ-Al_2O_3 (NiCeAl). The above catalyst compositions are optimal for this reaction [30–33]. Before the experiments, the catalysts were reduced with hydrogen (GHSV = 3000 h^{-1}, 450°C) for 8 h.

At a constant space velocity and invariable initial concentrations of carbon monoxide and hydrogen, the rate of methanation on the most active NiCaAl catalyst at 240°C did not depend on the rate of circulation; that is, external diffusion was not a limiting factor in the process. A change in the particle size of the catalysts from 0.31 to 3.0 mm also had no effect on the process; that is, the reaction was kinetically controlled.

An HP-PLOT column packed with molecular sieve 5 Å and a thermal-conductivity detector were used in the gas-chromatographic analysis of CO, and an HP-1 capillary column with dimethylpolysiloxane and a flame-ionization detector were used in the determination of methane and hydrocarbons.

RESULTS AND DISCUSSION

The analysis of the reaction mixture showed that CH_4 and H_2O are the only reaction products. The temperature dependence of the rate of methanation (r) in the Arrhenius coordinates ($\ln r$–$1/T$) at a constant composition of the reaction mixture is nonlinear; this fact is indicative of a fractional rational rather than power form of the rate equation (Fig. 1).

Figure 2 shows the dependence of the rate of the reaction at 240°C and constant initial conditions on the CO conversion (so-called conversion curves). The curves recorded at the other temperatures have the same shape. The curves for the NiCaAl and NiCeAl catalysts are convex, whereas the curves for the NiTi and NiAl pass through a small maximum. These shapes of the conversion curves suggest that the reaction is more strongly inhibited by the parent substances than by the products [34]. Bashkirova and Kiperman [34] also demonstrated that the rate equation can be invariable even if the shape of the conversion curve changes.

Because CH_4 and H_2O form in equimolar quantities, it is impossible to separately determine the influence of either product on the reaction rate. In order to clarify this issue, it is necessary to gain data on the reaction rate at different ratios between CH_4 and H_2O in the reaction mixture. For this purpose, different quantities of CH_4 and H_2O were added to the initial

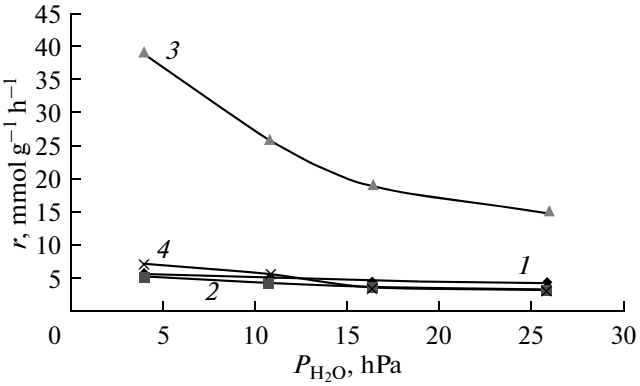

Fig. 3. Dependence of the reaction rate on the partial pressure of water vapor at 220°C, $P_{H_2} = 200$ hPa, and $P_{CO} = 6.0$ hPa for the following catalysts: (*1*) NiTi, (*2*) NiAl, (*3*) NiCaAl, and (*4*) NiCeAl.

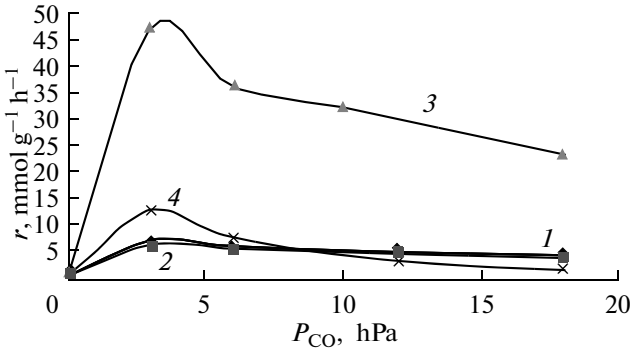

Fig. 4. Dependence of the reaction rate on the partial pressure of CO at 220°C and $P_{H_2} = 200$ hPa for the following catalysts: (*1*) NiTi, (*2*) NiAl, (*3*) NiCaAl, and (*4*) NiCeAl.

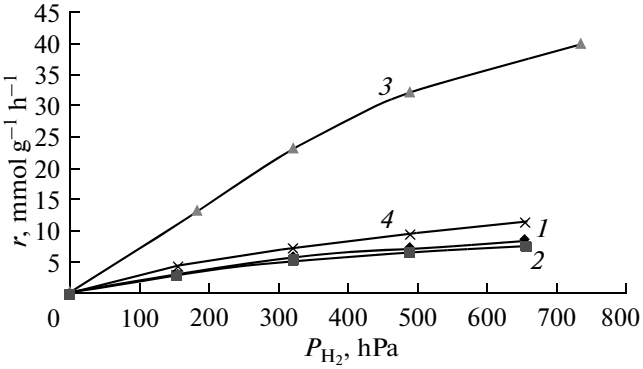

Fig. 5. Dependence of the reaction rate on the partial pressure of hydrogen at 220°C, $P_{CO} = 6$ hPa, and $P_{H_2O} = 4.0$ hPa for the following catalysts: (*1*) NiTi, (*2*) NiAl, (*3*) NiCaAl, and (*4*) NiCeAl.

mixture. Data analysis showed that CH_4 has no effect on the reaction rate, whereas an increase in the concentration of water vapor leads to a decrease in the reaction rate (Fig. 3). Consequently, the partial pressure of water vapor should enter into the denominator of the rate equation.

Figure 4 shows the dependence of the reaction rate on the partial pressure of CO at constant concentrations of the other reaction components. The curve has a maximum at low P_{CO} (~3.5 hPa). This fact suggests that the partial pressure of CO enters into both the numerator and the denominator of the rate equation, and the power in the denominator is higher than the power in the numerator [34].

The dependence of the reaction rate on the partial pressure of hydrogen at constant concentrations of the other reaction components (Fig. 5) indicates that r increses nonlinearly with an increasing hydrogen concentration. This also suggests that the partial pressure

Table 1. Kinetic data for CO methanation on the 37.5% $NiO/\gamma\text{-}Al_2O_3$ catalyst

T, °C	x, %	P_{CO}	P_{H_2}	P_{H_2O}	P_{CH_4}	r_{exp}	r_{calc}	Δ, %
		hPa				$mmol\ g^{-1}\ h^{-1}$		
180	23.8	3.8	329	1.2	1.2	1.06	0.67	37.3
	6.2	28.1	327	1.9	1.9	0.56	0.36	35.0
	12.1	8.8	329	1.2	1.2	0.81	0.68	16.6
	16.5	8.4	328	1.6	1.6	0.74	0.56	24.5
	14.6	8.5	329	1.5	1.5	0.65	0.60	7.3
200	52.4	4.8	651	5.2	5.2	3.51	3.72	5.9
	20.1	8.0	661	2.0	2.1	3.59	4.14	15.2
	18.1	8.2	495	1.8	1.8	3.23	3.95	22.3
	11.5	8.9	497	1.2	1.2	4.11	3.96	3.7
	7.85	27.6	326	2.4	2.4	1.40	1.76	25.5
	12.9	8.7	329	1.3	1.3	3.46	3.63	5.1
	10.5	9.0	330	1.0	1.0	3.75	3.62	3.4
	18.3	8.2	327	23.7	1.8	1.63	1.76	7.4
	10.7	18.0	327	2.1	2.1	1.91	2.40	26.0
	16.8	8.3	328	8.5	1.7	2.25	2.82	25.4
220	71.9	2.8	645	7.2	7.2	6.42	5.27	17.9
	41.5	5.8	654	4.2	4.2	7.41	6.27	15.4
	79.0	2.1	476	7.9	7.9	5.29	4.59	13.2
	60.9	3.9	482	6.1	6.1	5.44	5.71	5.0
	36.3	6.4	489	3.6	3.6	6.48	5.98	7.7
	26.6	7.3	492	2.7	2.7	7.13	5.93	16.7
	86.7	1.3	307	8.7	8.7	3.87	3.54	8.5
	65.5	3.4	314	6.6	6.6	4.39	5.26	19.8
	39.4	6.1	321	3.9	3.9	5.28	5.49	4.0
	21.2	7.9	327	2.1	2.1	5.68	5.32	6.2
	20.9	7.9	161	2.1	2.1	3.73	4.32	15.8
	63.7	1.8	323	3.2	3.2	5.69	5.87	3.2
	37.7	3.1	327	1.9	1.9	6.73	6.81	1.2
	58.8	8.2	298	11.8	11.8	3.50	3.80	8.8
	42.8	11.4	307	8.6	8.6	3.82	3.68	3.9
	31.8	20.4	304	9.6	9.6	2.84	2.57	9.5
	23.8	22.9	312	7.1	7.1	3.19	2.49	21.9
	75.0	2.5	310	14.3	7.5	3.35	3.38	0.79
	46.3	5.4	319	11.4	4.6	4.13	4.24	2.6
	25.6	7.4	325	9.4	2.6	4.57	4.31	5.7
	17.3	8.3	328	8.5	1.7	4.63	4.29	7.4
	54.3	4.6	317	17.8	5.4	3.64	3.37	7.5
	22.0	7.8	326	14.6	2.2	3.93	3.67	6.7
	55.0	4.5	316	27.4	5.5	2.46	2.46	0.36
	37.1	6.3	322	25.6	3.7	3.31	2.74	17.15
	25.4	7.5	325	24.4	2.5	3.40	2.84	16.4
	11.7	8.8	329	23.1	1.2	3.13	2.91	7.2
	30.1	7.0	324	3.0	13.0	5.38	5.42	0.76
	30.0	7.0	324	3.0	23.0	5.38	5.42	0.76
	30.10	7.0	324	3.0	33.0	5.38	5.42	0.76

Table1. (Contd.)

T, °C	x, %	P_{CO}	P_{H_2}	P_{H_2O}	P_{CH_4}	r_{exp}	r_{calc}	Δ, %
		hPa				mmol g^{-1} h^{-1}		
240	86.9	1.3	641	8.7	8.7	15.5	12.8	17.7
	82.1	1.8	475	8.2	8.2	14.7	14.0	4.2
	68.1	3.2	313	6.8	6.8	12.2	13.5	10.7
	52.1	4.8	484	4.8	4.8	17.0	14.7	13.3
	94.4	0.56	305	9.4	9.4	8.43	8.92	5.8
	45.0	5.5	320	4.5	4.5	12.0	11.5	4.65
	15.9	8.4	328	1.6	1.6	11.4	9.4	17.4
	28.2	7.2	158	2.8	2.8	7.55	7.97	5.5
	69.8	1.5	322	3.5	3.5	12.5	15.6	25.2
	88.3	1.2	306	30.7	8.8	7.88	6.78	14.0
	62.3	3.8	314	28.1	6.2	8.34	8.99	7.8
	90.0	1.0	306	21.4	9.0	8.04	8.05	0.16
	63.6	3.6	314	18.8	6.4	8.52	10.5	23.3
	71.3	2.9	312	13.9	7.1	9.55	11.8	24.1

of hydrogen enters into both the numerator and denominator of the reaction rate equation.

Tables 1–4 list kinetic data for CO methanation on nickel catalysts. It follows from these experimental data that, in general form, the rate of CO methanation on NiTi, NiAl, NiCaAl, and NiCeAl is described by the following equation:

$$r = \frac{k_1 P_{CO}^{l_1} P_{H_2}^{m_1}}{\left(k_2 P_{H_2}^{m_2} + k_3 P_{CO}^{l_2} + k_4 P_{H_2O}^{n}\right)^{2\alpha}}, \qquad (1)$$

where k_1–k_4 are constants and α is the linearity ratio coefficient.

Computer-aided calculation of the kinetic data given in Tables 1–4 showed that Eq. (1) provides the best fit to these data at $l_1 = l_2 = 1$, $m_1 = m_2 = 0.5$, $n = 1$, and $\alpha = 1$; therefore,

$$r = \frac{k_1 P_{CO} P_{H_2}^{0.5}}{\left(k_2 P_{H_2}^{0.5} + k_3 P_{CO} + k_4 P_{H_2O}\right)^2}. \qquad (2)$$

Table 5 presents the numerical values of the constants, taking into account all of the experimental data, and also specifies the root-mean-square deviations of the calculated rates of CO methanation from their experimental values (Δ). The linear dependence of $1/r^{0.5}$ on P_{H_2O} at constant P_{CO} and P_{H_2} demonstrates that P_{H_2O} to the first power enters into the denominator of the rate equation at $\alpha = 1$ (Fig. 6). The value of $\alpha = 1$ corresponds to the proceeding of the reaction at high adsorbate coverages of the surface.

The numerical values of the constants show that CO is adsorbed more strongly than hydrogen. The ratio k_2/k_3 at 220°C for the nickel catalysts supported on Al_2O_3 varies in the range from 0.12 to 0.14. The introduction of Ca or Ce into the NiAl catalyst weakens the adsorption of water vapor, which substantially increases the activity of the catalyst containing Ca. The rates of CO methanation on NiTi and NiAl are similar; however, on a Ni atom basis, they are higher for the former catalyst.

In an earlier study [29] the reaction mechanism of CO methahation was investigatedusing isotopic and unsteady-state methods and the following step-by-step reaction scheme was proposed for the nickel catalysts (Z is an active surface site):

(1) $H_2 + Z = 2HZ$,

(2) $CO + Z = [CO]Z$,

(3) $[CO]Z + HZ = [COH]Z + Z$,

(4) $[COH]Z + HZ = [HCOH]Z + Z$,

Table 2. Kinetic data for CO methanation on the 7.5% NiO/TiO_2 catalyst

T, °C	x, %	P_{CO}	P_{H_2}	P_{H_2O}	P_{CH_4}	r_{exp}	r_{calc}	Δ, %
		hPa				mmol g^{-1} h^{-1}		
180	13.7	8.6	663	1.4	1.4	1.22	0.90	26.1
	12.3	8.8	496	1.2	1.2	1.1	0.93	15.9
	37.9	6.2	322	3.8	3.8	0.85	0.78	8.4
	14.7	8.5	329	1.5	1.5	0.98	0.92	6.7
	13.6	4.3	331	0.7	0.7	0.91	0.83	8.7
	8.5	4.6	332	0.43	0.43	1.14	0.86	24.5
	10.0	27.0	324	3.0	3.0	0.67	0.68	2.2
	13.5	8.6	329	1.4	1.4	0.90	0.92	2.8
	26.5	7.4	325	2.6	2.6	0.89	0.85	4.0
	10.8	8.9	330	1.1	1.1	0.89	0.94	5.1
	8.6	9.1	164	0.86	0.86	0.77	0.91	18.6
	18.5	4.1	330	0.93	0.93	0.83	0.80	3.7
	12.0	17.6	326	2.4	2.4	0.80	0.82	1.9
	13.8	8.6	329	1.4	1.4	0.92	0.92	0.37
200	20.2	8.0	661	2.0	2.0	3.61	2.71	24.8
	30.4	7.0	491	3.0	3.0	2.71	2.62	3.5
	15.7	8.4	495	1.6	1.6	2.80	2.64	5.6
	23.8	22.9	312	7.1	7.1	1.59	1.39	12.7
	29.2	14.2	316	5.8	5.8	1.96	1.84	6.0
	15.4	16.9	324	3.0	3.0	2.06	1.77	13.8
	50.1	5.0	318	5.0	5.0	2.24	2.41	7.7
	26.6	7.3	325	2.7	2.7	2.38	2.50	5.2
	20.3	4.0	330	1.0	1.0	2.72	2.78	2.2
	25.7	7.4	325	24.5	2.6	1.72	1.45	15.5
	22.1	7.8	326	9.0	2.2	1.97	2.09	5.7
	18.4	8.2	327	23.7	1.8	1.64	1.48	9.6
	26.9	7.3	325	15.1	2.7	1.80	1.80	0.11
	14.1	8.5	329	13.8	1.4	1.89	1.84	2.8
	27.8	7.2	325	9.6	2.8	1.86	2.07	11.3
	17.9	8.2	328	1.8	1.8	2.40	2.49	3.9
	15.5	8.4	328	1.6	1.6	2.77	2.49	10.2
220	62.0	3.8	648	6.2	6.2	8.30	6.80	18.1
	51.2	4.9	485	5.1	5.1	6.86	6.47	5.6
	18.9	8.1	494	1.9	1.9	6.75	5.68	15.8
	32.1	6.8	323	3.2	3.2	5.73	5.44	5.1
	20.9	7.9	161	2.1	2.1	3.73	4.11	10.0
	51.2	2.4	325	2.6	2.6	6.86	7.19	4.8
	23.8	3.8	329	1.2	1.2	6.38	7.03	10.2
	59.0	8.2	298	11.8	11.8	3.95	4.30	8.9
	51.9	14.4	286	15.6	15.6	3.48	2.97	14.5
	69.5	3.0	312	13.8	7.0	4.65	5.33	14.7
	37.6	6.2	322	10.6	3.8	5.04	5.02	0.38
	19.0	8.1	327	8.7	1.9	5.09	4.64	8.9

Table 2. (Contd.)

T, °C	x, %	P_{CO}	P_{H_2}	P_{H_2O}	P_{CH_4}	r_{exp}	r_{calc}	Δ, %
		hPa				mmol g^{-1} h^{-1}		
220	64.3	3.6	314	18.8	6.4	4.31	4.78	10.9
	35.5	6.4	322	15.9	3.6	4.75	4.58	3.7
	17.3	8.3	328	14.1	1.7	4.63	4.29	7.5
	60.8	3.9	315	28.0	6.1	4.07	4.03	1.1
	33.3	6.7	323	25.2	3.3	4.46	3.98	10.7
	16.2	8.4	328	23.5	1.62	4.34	3.81	12.2
	41.8	5.8	320	4.2	14.2	5.60	5.72	2.2
	41.8	5.8	320	4.2	34.2	5.60	5.72	2.2
	58.9	4.1	315	5.9	5.9	5.26	6.17	17.2
	14.1	8.6	329	1.4	1.4	5.04	4.95	1.6
	74.8	2.5	478	7.5	7.5	6.68	6.39	4.3
	39.0	6.1	488	3.9	3.9	6.96	6.20	11.0
	13.8	8.6	163	1.4	1.4	3.70	3.94	6.5
	72.3	1.4	322	3.6	3.6	6.46	6.44	0.19
240	86.4	1.4	474	8.6	8.6	15.4	16.0	3.9
	75.4	2.5	477	7.5	7.5	20.2	15.9	21.0
	60.6	3.9	315	6.1	6.1	10.8	12.6	16.5
	40.6	5.9	321	4.1	4.1	10.9	10.2	5.9
	26.8	7.3	325	2.7	2.7	9.57	9.04	5.6
	93.4	0.66	305	9.3	9.3	12.5	13.3	6.0
	81.1	1.9	309	8.1	8.1	14.5	15.4	6.7
	51.4	4.9	318	5.1	5.1	13.8	11.4	17.1
	68.9	3.1	312	19.3	6.9	12.3	11.7	5.3
	76.1	2.4	310	14.4	7.6	13.6	13.3	2.2
	22.2	7.8	160	2.2	2.2	5.95	6.60	10.8
	83.5	3.3	283	16.7	16.7	11.4	11.5	1.3
	84.3	1.6	308	30.3	8.4	11.3	10.3	9.1
	59.9	4.0	315	27.9	6.0	10.7	9.79	8.5

Table 3. Kinetic data for CO methanation on the (37.5% NiO + 10.2% CaO)/γ-Al_2O_3 catalyst

T, °C	x, %	P_{CO}	P_{H_2}	P_{H_2O}	P_{CH_4}	r_{exp}	r_{calc}	Δ, %
		hPa				mmol g^{-1} h^{-1}		
180	53.0	7.0	476	8.0	8.0	4.89	5.25	7.5
	22.0	11.7	490	3.3	3.3	6.09	6.08	0.15
	12.0	13.2	495	1.8	1.8	6.64	6.19	6.8
	17.0	12.4	492	14.9	2.6	4.18	3.48	17.7
	8.0	13.8	496	23.1	1.2	2.95	2.58	12.5
	19.0	16.2	189	3.8	3.8	3.11	3.42	9.9
	13.0	17.4	192	2.6	2.6	3.20	3.46	8.2
	50.0	10.0	470	10.0	10.0	4.10	4.44	8.3
	11.0	17.8	493	2.2	2.2	5.41	5.04	6.9
	17.0	12.4	492	2.6	12.6	6.27	6.14	2.1
	11.0	13.4	495	14.0	1.6	4.06	3.57	12.0
	48.0	5.2	471	4.8	4.8	5.90	6.77	14.7
200	83.0	2.6	463	12.4	12.4	7.65	7.06	7.7
	47.0	8.0	479	7.0	7.0	13.0	12.3	5.7
	35.0	9.8	484	5.2	5.2	12.9	12.8	0.84
	18.0	12.3	492	2.7	2.7	13.3	13.1	1.1
	11.0	13.4	495	1.6	1.6	12.2	13.2	8.3
	55.0	4.5	467	5.5	5.5	13.5	14.1	4.4
	41.0	5.9	475	4.1	4.1	15.1	15.5	2.4
	15.0	17.0	491	3.0	3.0	11.1	10.8	2.6
	14.0	17.2	192	2.8	2.8	6.89	7.47	8.5
	9.00	18.2	194.6	1.8	1.8	6.64	7.48	12.6
	61.0	5.8	473	9.2	19.2	11.2	11.1	1.4
	43.0	8.5	481	6.4	16.4	11.9	12.5	4.9
	14.0	12.9	494	14.5	2.1	7.75	8.12	4.8
	11.0	13.4	495	23.6	1.6	6.09	6.06	0.48
220	76.0	4.8	704	15.2	15.2	18.7	18.4	1.6
	89.0	2.2	447	17.8	17.8	10.9	10.2	6.4
	73.0	5.4	456	14.6	14.6	18.0	17.4	2.8
	60.0	8.0	464	12.0	12.0	22.1	20.1	9.2
	51.0	9.8	469	10.2	10.2	25.1	21.1	16.1
	44.0	11.2	304	5.5	8.8	21.6	21.0	2.8
	20.0	16.0	188	4.0	4.0	14.8	15.2	3.0
	93.0	1.0	458	14.0	14.0	8.58	8.07	5.9
	73.0	4.0	467	10.9	10.9	20.2	20.2	0.03
	73.0	1.3	489	3.6	3.6	26.9	24.5	8.9
	39.0	3.0	494	2.0	2.0	33.6	37.9	13.0
	87.0	1.3	448	8.7	8.7	16.05	14.38	10.39
	69.0	3.1	459	6.9	6.9	21.2	24.8	17.2
	49.0	5.1	471	4.9	4.9	27.1	30.2	11.5
	38.0	6.2	477	3.8	3.8	28.0	31.7	13.1
	75.0	7.5	432	22.5	22.5	13.8	13.0	6.1
	75.0	3.8	466	18.0	11.2	13.8	13.3	3.7
	53.0	7.0	476	14.8	8.0	19.6	18.0	7.7
	40.0	9.0	482	12.8	6.0	22.1	19.4	12.2
	67.0	5.0	470	22.4	10.0	12.4	12.1	2.3
	44.0	8.4	480	19.0	6.6	16.2	15.4	5.0
	30.0	10.5	486	16.9	4.5	16.6	16.5	0.51
	24.0	11.4	489	16.0	3.6	17.7	16.8	4.8
	34.0	9.9	485	27.0	5.1	12.5	12.0	4.1
	74.0	3.9	467	11.1	26.1	20.5	19.8	3.1
	92.0	1.2	459	13.8	33.8	8.48	9.00	6.1
	65.0	5.2	471	9.8	29.8	24.0	22.6	5.9

Table 3. (Contd.)

T, °C	x, %	P_{CO}	P_{H_2}	P_{H_2O}	P_{CH_4}	r_{exp}	r_{calc}	Δ, %
		hPa				mmol g^{-1} h^{-1}		
240	72.0	4.2	468	10.8	10.8	44.3	41.2	7.0
	55.0	6.8	475	8.25	8.25	50.7	47.9	5.6
	38.0	9.3	483	5.7	5.7	56.1	50.0	10.8
	27.0	11.0	488	4.0	4.0	59.8	50.2	16.0
	70.0	6.0	458	14.0	14.0	34.4	36.9	7.3
	60.0	8.0	464	12.0	12.0	44.3	40.0	9.6
	28.0	14.4	183	5.6	5.6	27.5	29.5	7.1
	76.0	3.6	466	23.8	11.4	21.0	21.2	1.1
	56.0	6.6	475	20.8	8.4	31.0	29.0	6.5
	70.0	4.5	468	30.5	10.5	19.4	18.3	5.5
	49.0	7.6	478	27.3	7.4	27.1	24.0	11.4

(5) $[HCOH]Z + Z = [CH]Z + [OH]Z$,

(6) $[CH]Z + HZ = [CH_2]Z + Z$,

(7) $[CH_2]Z + HZ = [CH_3]Z + Z$,

(8) $[CH_3]Z + HZ = CH_4 + 2Z$,

(9) $[OH]Z + HZ = [H_2O]Z + Z$,

(10) $[H_2O]Z = H_2O + Z$.

The observation of a kinetic isotope effect [29] suggests that steps (3) and (4) can be slow. The above rate equation is consistent only with the assumption that step (3) is slow. If the reaction proceeds at high adsorbate coverages of the surface, a rate equation identical to the equation found experimentally [28] follows from the step-by-step reaction scheme.

Thus, we studied the kinetics of CO methanation on different nickel catalysts and found that the experimental data can be described by the same rate equation. We determined the slow step of the process and

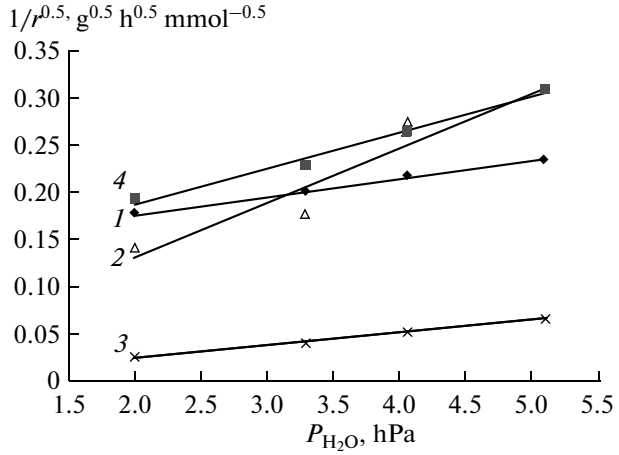

Fig. 6. Dependence of $1/r^{0.5}$ on P_{H_2O} at 220°C, P_{H_2} = 200 hPa, and P_{CO} = 6.0 hPa for the following catalysts: (*1*) NiTi, (*2*) NiAl, (*3*) NiCaAl, and (*4*) NiCeAl.

Table 4. Kinetic data obtained in the study of the reaction of CO methanation on the (37.5% NiO + 0.1% Ce_2O_3)/γ-Al_2O_3 catalyst

T, °C	x, %	P_{CO}	P_{H_2}	P_{H_2O}	P_{CH_4}	r_{exp}	r_{calc}	Δ, %
		hPa				mmol g^{-1} h^{-1}		
180	49.8	5.0	318	5.0	5.0	1.1	1.2	7.0
	27.0	7.3	325	2.7	2.7	1.2	1.4	12.4
	19.8	8.0	327	2.0	2.0	1.3	1.4	4.6
	10.1	9.0	330	1.0	1.0	1.35	1.42	4.8
	18.0	8.2	328	1.8	1.8	1.21	1.39	15.6
	10.5	4.5	331	0.53	0.53	1.41	1.51	7.1
	19.3	16.1	321	3.9	3.9	0.86	1.06	23.2
	16.2	8.4	328	8.4	1.6	1.08	1.06	1.6
	9.5	9.0	330	22.9	0.95	0.64	0.67	5.0
200	29.2	7.1	491	2.9	2.9	3.91	3.85	1.6
	17.6	8.2	495	1.8	1.8	4.71	3.86	18.0
	49.1	5.1	318	4.9	4.9	3.29	3.48	5.9
	36.0	6.5	322	3.6	3.6	3.62	3.57	1.4
	27.0	7.3	325	2.7	2.7	3.62	3.58	1.1
	13.0	8.7	329	1.3	1.3	3.48	3.55	1.8
	40.3	3.0	327	2.0	2.0	4.05	4.03	0.53
	28.2	3.6	329	1.4	1.4	3.78	4.23	11.9
	20.0	8.0	327	8.8	2.0	2.67	2.83	5.8
	31.0	6.9	324	15.5	3.1	2.07	2.31	11.9
	17.0	8.3	328	14.1	1.7	2.28	2.39	4.9
	25.6	7.4	325	24.5	2.6	1.71	1.79	4.6
	15.0	8.5	328	23.4	1.5	2.00	1.85	7.4
220	69.9	3.0	646	6.9	6.9	9.36	8.95	4.4
	42.2	5.8	654	4.2	4.2	11.3	9.72	14.0
	25.1	3.75	329	1.25	1.25	6.71	8.04	19.7
	78.4	2.2	476	7.8	7.5	7.87	7.85	0.34
	44.7	5.5	487	4.5	4.5	8.99	9.21	2.5
	37.1	6.3	489	3.7	3.7	9.93	9.11	8.3
	26.0	7.4	492	2.6	2.6	10.47	8.89	15.1
	30.3	7.0	324	3.0	3.7	8.11	8.07	0.47
	16.3	8.4	328	1.6	2.3	8.72	7.70	11.7
	88.1	2.4	280	17.6	16.5	3.93	4.71	19.7
	62.4	7.5	300	12.5	9.5	5.57	5.80	4.0
	31.6	13.7	314	6.3	5.9	5.63	5.09	9.6
	53.8	13.8	284	16.2	16.2	3.61	4.10	13.8
	39.7	18.1	297	11.9	11.9	3.98	3.81	4.3
	29.9	21.0	306	9.0	9.0	4.00	3.62	9.5
	75.8	2.4	310	14.4	7.6	5.07	5.59	10.2
	30.6	6.9	324	9.9	3.1	6.14	6.57	7.0
	15.8	8.4	328	8.4	1.6	6.37	6.40	0.52
	89.0	1.1	306	21.3	8.9	2.98	2.75	7.85
	83.0	1.7	308	30.2	8.3	2.78	2.50	10.1
	71.8	2.8	311	29.1	7.2	3.20	3.36	4.8
240	93.1	0.65	472	9.4	9.4	12.5	11.8	5.6
	81.3	1.9	476	8.1	8.1	21.8	19.6	10.0
	89.4	1.1	306	8.9	8.9	12.0	15.2	27.3
	80.4	2.0	309	8.0	8.0	16.2	18.6	15.1
	69.3	3.1	312	6.9	6.9	18.6	19.2	3.6
	53.1	4.7	317	5.3	5.3	21.3	18.2	14.9
	42.0	5.8	320	4.2	4.2	22.5	17.1	24.0
	72.3	2.8	311	19.6	7.2	9.68	11.8	21.7
	42.7	5.7	320	26.2	4.3	8.57	9.85	14.9
	31.0	6.9	324	25.0	3.1	8.30	9.78	17.8

Table 5. Constants of Eq. (2) and the root-mean-square deviations of calculated reaction rates from experimental values

Catalyst	k_1, mmol $g^{-1} h^{-1} hPa^{-1.5}$	k_2, $hPa^{-0.5}$	k_3, hPa^{-1}	k_4, hPa^{-1}	Δ, %
NiTi	$9.90 \times 10^1 e^{-0.56/T}$	$1.82 \times 10^{-9} e^{9684/T}$	$1.23 \times 10^{-1} e^{1837/T}$	$8.66 \times 10^{-12} e^{12063/T}$	20
NiAl	$6.00 \times 10^4 e^{-2483/T}$	$6.30 \times 10^{-2} e^{1505/T}$	$2.00 \times 10^{-2} e^{3018/T}$	$8.67 \times 10^{-18} e^{19627/T}$	25
NiCaAl	$4.55 \times 10^2 e^{-3117/T}$	$6.91 \times 10^{-4} e^{1766/T}$	$1.02 \times 10^{-3} e^{2549/T}$	$1.02 \times 10^{-5} e^{4251/T}$	17
NiCeAl	$6.02 \times 10^2 e^{-1549/T}$	$5.18 \times 10^{-8} e^{7587/T}$	$1.60 \times 10^{-2} e^{2386/T}$	$8.20 \times 10^{-7} e^{6345/T}$	18

evaluated the role of the support and calcium and cerium dopants in nickel catalysts.

ACKNOWLEDGMENTS

This study was supported by the Russian Foundation for Basic Research and the Vietnamese Academy of Science and Technology (grant no. 09-03-90301 Viet_a).

REFERENCES

1. Vlasenko, V.M. and Yuzefovich, G.E., *Usp. Khim.*, 1969, vol. 38, no. 9, p. 1622.
2. Vlasenko, V.M., Yuzefovich, G.E., and Rusov, M.T., *Kinet. Katal.*, 1965, vol. 6, no. 4, p. 688.
3. Kreindel', A.I., Sobolevskii, V.S., Golosman, E.Z., and Yakerson, V.I., *Kinet. Katal.*, 1974, vol. 15, no. 2, p. 408.
4. Kon'on, Zh.-M. and Margaren, Zh., *Kinet. Katal.*, 1975, vol. 16, no. 6, p. 1552.
5. Sehested, J., Dahl, S., Jacobsen, J., and Rostrup-Nielsen, J.R., *J. Phys. Chem. B*, vol. 109, no. 6, p. 2432.
6. Vannice, M.A., *Catal. Rev. Sci. Eng.*, 1976, vol. 14, no. 2, p. 1.
7. Ekert, J.G. and Bell, A.T., *J. Catal.*, 1979, vol. 58, no. 1, p. 170.
8. Jacobs, P.A. and Nijs, H.H., *J. Catal.*, 1980, vol. 64, no. 2, p. 251.
9. Ross, J.R.H., *J. Catal.*, 1981, vol. 71, no. 1, p. 205.
10. Mori, M., Masuda, H., Imai, H., Miyamoto, A., Baba, S., and Murakami, Y., *J. Phys. Chem.*, 1982, vol. 86, no. 14, p. 2753.
11. Polizzoti, R.S. and Schwarz, J.A., *J. Catal.*, 1982, vol. 77, no. 1, p. 1.
12. Dalmon, J.A. and Martin, G., *J. Catal.*, 1983, vol. 84, no. 1, p. 45.
13. Hayes, R.E., Thomas, W.J., and Hayes, K.E., *J. Catal.*, 1985, vol. 92, no. 2, p. 312.
14. Alstrup, I., *J. Catal.*, 1995, vol. 151, no. 1, p. 216.
15. Ho, S.V. and Harriott, P., *J. Catal.*, 1980, vol. 64, no. 2, p. 272.
16. Schoubye, P., *J. Catal.*, 1969, vol. 14, no. 3, p. 238.
17. Huang, C.P. and Richardson, J.T., *J. Catal.*, 1978, vol. 51, no. 1, p. 1.
18. Meerten, R.Z.C., Vollenbrock, J.G., Croon, M.H.J.M., Nisselrooy, P.F.M.T., and Coenen, J.W.E., *Appl. Catal.*, 1982, vol. 3, no. 1, p. 29.
19. Klose, J. and Baerns, M., *J. Catal.*, 1984, vol. 85, no. 1, p. 105.
20. Coenen, J.W.E., Nisselrooy, P.F.M.T., Croon, M.H.J.M., Dooren, P.F.H.A., and Meerten, R.Z.C., *Appl. Catal.*, 1986, vol. 25, no. 1, p. 1.
21. Mey, F., Spinder, H., Rohlander, W., and Wejbenborn, H., *Chem. Tech.*, 1986, vol. 38, no. 7, p. 300.
22. Demmin, R.A. and Gorte, R.J., *J. Catal.*, 1987, vol. 105, no. 2, p. 373.
23. Ibraeva, Z.A., Nekrasov, N.V., Yakerson, V.I., Gudkov, B.S., Golosman, E.Z., Beisembaeva, Z.T., and Kiperman, S.L., *Kinet. Katal.*, 1987, vol. 28, no. 2, p. 386.
24. Yadav, R. and Rinker, R.G., *Can. J. Chem. Eng.*, 1993, vol. 71, no. 3, p. 202.
25. Kopyscinski, J., Schidhauer, T.J., Vogel, F., Biollaz, S.M.A., and Wokaun, A., *J. Catal.*, 2010, vol. 271, no. 2, p. 262.
26. Stytsenko, V.D., Apostol, E.S., and Rozovskii, A.Ya., *Tezisy dokl. Vses. konf. "Khimicheskie sintezy na osnove odnouglerodnykh molekul"* (Proc. All-Union Conf. on Chemical Syntheses Based on Single-Carbon Molecules), Moscow, 1987, p. 24.
27. Stytsenko, V.D., *Zh. Prikl. Khim.*, 1990, vol. 63, no. 4, p. 933.
28. Kiperman, S.L., *Vvedenie v kinetiku geterogennykh kataliticheskikh reaktsii* (Introduction to the Kinetics of Heterogeneous Catalytic Reaxctions), Moscow: Nauka, 1964.
29. Luu Cam Loc, Nguyen Manh Huan, Gaidai, N.A., Ho Si Thoang, Nekrasov, N.V., Agafonov, Yu.A., and Lapidus, A.L., *Kinet. Catal.*, 2011, vol. 52, no. 5, p. 749.
30. Loc, L.C., Huan, N.M., Dung, N.K., Phuc, N.H., and Thoang, H.S., *Adv. Nat. Sci.*, 2006, vol. 7, nos. 1–2, p. 91.
31. Huan, N.M., Loc, L.C., and Dung, N.K., *J. Chem.*, 2007, vol. 45, no. 2, p. 169.
32. Loc, L.C. and Huan, N.M., *J. Chem.*, 2007, vol. 45, no. 1, p. 33.
33. Huan, N.M., Loc, L.C., Dung, N.K., and Thoang, H.S., *Adv. Nat. Sci.,* 2008, vol. 9, no. 1, p. 69.
34. Bashkirova, S.G. and Kiperman, S.L., *Kinet. Katal.*, 1970, vol. 11, no. 3, p. 631.